nature astronomy

Article

https://doi.org/10.1038/s41550-025-02725-1

Multiple outflows and delayed ejections revealed by early imaging of novae

Received: 13 July 2025

Accepted: 28 October 2025

Published online: 5 December 2025

Check for updates

A list of authors and their affiliations appears at the end of the paper

Novae are thermonuclear eruptions on accreting white dwarfs in interacting binaries. Although most of the accreted envelope is expelled, the mechanism—impulsive ejection, multiple outflows or prolonged winds, or a common-envelope interaction—remains uncertain. Gigaelectronvolt γ-ray detections from >20 Galactic novae establish these eruptions as nearby laboratories for shock physics and particle acceleration, underscoring the need to determine how novae eject their envelopes. Here we report on near-infrared interferometry, supported by multiwavelength observations, of two γ-ray-detected novae. The images of the very fast 2021 nova V1674 Her, taken just 2–3 days after discovery, reveal the presence of two perpendicular outflows. The interaction between these outflows probably drives the observed γ-ray emission. Conversely, the images of the very slow 2021 nova V1405 Cas suggest that the bulk of the accreted envelope was ejected more than 50 days after the eruption began, as the nova slowly rose to its visible peak, during which the envelope engulfed the system in a common-envelope phase. These images offer direct observational evidence that the mechanisms driving mass ejection from the surfaces of accreting white dwarfs are not as simple as previously thought, revealing multiple outflows and delayed ejections.

A classical nova is a transient astronomical event characterized by sudden dramatic brightening of an interacting binary star system, resulting from a thermonuclear runaway on the surface of a white dwarf that has accreted hydrogen-rich material from its companion[1,2]. The energy released by the thermonuclear runaway causes the accreted envelope to expand tremendously, although this energy alone may not be sufficient for completely ejecting it from the binary system[3]. As novae are observed to expel material at velocities ranging from approximately 500 to 10,000 km s^{-1} (refs. 4,5), some additional mechanism might be at work. The possibilities include multiple outflows and winds powered by continuing nuclear burning on the white dwarf[5–8], and/or expulsion through a common-envelope interaction drawing energy from the orbital motion of the binary companion[9,10]. Understanding how novae expel their envelopes has never been more important, given the now-routine detection of gigaelectronvolt (GeV) γ-ray emission from more than 20 Galactic novae by the Large Area Telescope (LAT) on the Fermi Gamma-Ray Space Telescope[11–14]. These detections have established novae as a new class of particle accelerators and confirmed the presence of strong, energetic shocks within the nova ejecta[15,16]. More recent studies showed that these shocks can contribute a substantial fraction of the nova luminosity, highlighting their importance in powering these enigmatic events[17,18]. The fact that the luminosity of some novae could be powered by shocks means that novae are particularly valuable laboratories to better understand the shock-powered transients, with substantial implications for other interaction-powered events such as super-luminous supernovae (for example, ref. 19), Type Ia-Circumstellar Medium supernovae (for example, ref. 20) and stellar mergers (for example, ref. 21).

The formation mechanisms of the energetic shocks that lead to the GeV γ-ray emission from novae are still poorly constrained. Recent models suggest that these shocks are internal to the nova ejecta; more specifically, they occur at the interface of multiple (at least two) ejections: an initial, slower ejection/outflow possibly directed towards the orbital plane due to the binary motion, followed by a faster outflow/

e-mail: eaydi@ttu.edu; monnier@umich.edu

wind that travels more freely in the polar directions—possibly driven by radiation powered by the near-Eddington luminosity of the nuclear burning white dwarf[3,5,10,16–18,22] (Fig. 1a). As these flows interact, they lead to the shocks responsible for particle acceleration and high-energy emission. This picture was first inspired by the radio imaging of the 2012 Fermi-detected nova V959 Mon (see fig. 2 in ref. 10), which showed evidence for two outflows expanding in orthogonal directions. This scenario garnered further support based on early spectroscopic follow-up of a large sample of novae by ref. 5, which showed consistent evidence for multiple spectral components, characterized by distinct velocities, and which were associated with multiple physically distinct ejections (see also refs. 4,6,7,22–27). If the binary motion indeed plays a role in expelling the nova envelope during the early stages of the eruption[3,10,28], by transferring angular momentum and energy to the ejecta, novae would become miniature common-envelope systems evolving in real time, that is, on observable timescales (days or weeks). This would make novae ideal laboratories in our Galactic backyard to constrain the physics of common-envelope interaction, which dictates the future evolution of more than 10% of stars[29], yet these processes remain poorly constrained observationally and uncertain theoretically (for example, refs. 30,31).

Decades of imaging of old nova shells show a clear departure from spherical symmetry in many novae, with diverse structures, including elliptical morphologies, rings, polar caps/knots and clumps[32–35]. While some of these structures could have been influenced by the binary companion and its role in shaping the ejecta[28], static images of nova remnants observed years to decades after eruption do not allow us to build a complete chronological picture of the ejecta's shaping and morphological evolution. High-resolution imaging taken during the early days of the eruption is necessary to better understand the ejection scenario in novae—a challenging task given the small size of the ejecta during these early stages (a few milliarcseconds projected on the sky). However, recent advances in optical/near-infrared (NIR) interferometry with facilities such as the Center for High Angular Resolution Astronomy (CHARA[36]) Array and the Very Large Telescope Interferometer[37,38], which are capable of resolving structures down to a few milliarcseconds (mas), now make it possible to observe nova ejecta during the early days of the eruption. Because some novae reach brighter than 5–6 magnitudes in the optical/NIR, they are ideal targets for such facilities. Previous efforts were carried out for some novae, such as the recurrent nova T Pyx (2011)[39], which revealed evidence for bipolar ejections, and the classical nova V339 Del[40], where the size of the early expanding fireball was measured. Here, we report on early (days to weeks) imaging of two Galactic Fermi-detected novae, namely V1674 Her and V1405 Cas (both erupted in 2021), obtained with the CHARA Array, revealing evidence for multiple and delayed ejections. These novae sample the two extremes of the nova population, with V1674 Her being one of the fastest novae ever observed and V1405 Cas evolving very slowly, staying near its peak brightness for around 200 days.

Nova V1674 Her (Nova Herculis 2021) was detected in eruption on 2021 June 12.19 UT (t_0) at a visible brightness of around 8.5 mag. It rose to peak very rapidly, reaching a maximum visible brightness of 6.0 mag in less than 16 h. It then declined by 2 magnitudes in around a day, making it one of the fastest evolving novae on record[41,42] (Supplementary Fig. 3). The nova was detected as a Fermi source during the first 2 days of the eruption, implying the presence of energetic shocks leading to high-energy GeV emission[42–44]. We obtained CHARA NIR interferometry for V1674 Her on UT 2021 June 14 and 15, with the Michigan Infra-Red Combiner-eXeter (MIRC-X) instrument[45], just approximately 2 and 3 days into the eruption (Fig. 1). The CHARA images show a clear deviation from spherical symmetry, with evidence for two ejecta components: (1) a bipolar outflow moving towards the northeast and southwest directions and expanding at a greater rate relative to (2) a central structure, with an ellipsoidal morphology, extended in the perpendicular direction compared with the other flow. This is in striking agreement with the multiple-ejections scenario suggested to explain the formation of shocks in novae. This is also consistent with the early spectroscopic follow-up of the nova, which revealed unusually high velocities for a classical nova—consistent with the rapid light curve evolution—and exhibiting two spectral components in the hydrogen Balmer lines: a premaximum P Cygni profile with an absorption trough at blueshifted velocity of around 3,800 km s^{-1}, and a broad emission that emerges around a day after peak, with absorption at blueshifted velocities of around 5,500 km s^{-1}—co-existing with the premaximum absorption (Fig. 1 and Supplementary Figs. 7 and 8). This spectral evolution is common in nova spectra as discussed in ref. 5, which associated these two components with physically distinct ejections or outflows (the full spectral evolution of V1674 Her is presented in Supplementary Figs. 4–6). These outflows will rapidly interact, leading to bright high-energy GeV emission[16], which was indeed a defining feature of nova V1674 Her during the first few days of the eruption[42]. Therefore, it is reasonable to suggest that the central ellipsoidal structure is associated with the premaximum P Cygni profile, while the rapidly expanding caps or outflow correspond to the faster spectral absorption component that emerged after the peak.

We use the PMOIRED tool to fit the V1674 Her visibilities and closure phases measured by the interferometer with different models approximating the nova image and to measure the projected size of the ejecta (for example, central component + elongated ring; see Supplementary Information for more detail). Based on these models, we measure angular radii of 0.90 ± 0.07 mas and 1.23 ± 0.11 mas for the faster component, in the first and second epochs, respectively (Supplementary Figs. 10 and 11 and Supplementary Table 2). We assume that the faster flow started expanding around the time the nova was first detected in γ-rays (the main tracer of the shocks between the slower and faster flows[5,18]), which started around $t = 0.5 \pm 0.5$ days. Using a velocity of 5,500 ± 500 km s^{-1} (measured from the optical spectra, as a proxy for the total expansion velocity), an expansion duration $\Delta(t) = 1.7 \pm 0.5$ days, a radius 0.90 ± 0.07 mas, and assuming we are observing the system at 67° inclination[46], we derive a distance $d \approx 5.5 \pm 1.7$ kpc towards V1674 Her (based on the expansion parallax). Similarly, using the second epoch (an angular radius of 1.23 ± 0.11 mas), an expansion duration $\Delta(t) = 2.7 \pm 0.5$ days, with the same assumptions, we derive a distance $d \approx 6.4 \pm 1.2$ kpc towards V1674 Her. These distances are consistent with distances derived from other methods (Supplementary Information and Supplementary Fig. 9). This implies that the association of the rapidly expanding ejecta component in the CHARA images with the faster spectral component in the Balmer lines is reasonable and supports our interpretation of the structures observed in the CHARA images.

Resolving the evolution and asymmetry of multiple ejecta components just 2–3 days into a nova event is remarkable. These images provide observational evidence that nova ejection is more complex than a single ballistic event, consistent with the multiple-outflow scenario, and offer valuable insights into the formation of shocks in novae.

The second case presented in this study is nova V1405 Cas, which was discovered on 2021 March 18.42 UT (t_0) at a visible brightness of 9.6 mag, and is the extreme opposite of V1674 Her, given its slow evolution. The nova reached a V-band magnitude of approximately 7.5 a few days after discovery. Thereafter, the brightness increase halted for a couple of weeks, before rising again to reach a peak in the V-band of 5.1 mag around 53 days after its initial discovery (Fig. 2). During this phase (which is often referred to as the premaximum halt), the optical spectral lines exhibited P Cygni profiles characterized by shallow absorptions and velocities that initially measured around 1,500 km s^{-1} but rapidly decreased to about 700 km s^{-1} (Fig. 2b and Supplementary Figs. 20 and 24). This apparent deceleration is probably the result of decreasing opacity in the ejecta[5,47]. The presence of shallow absorptions and the rapid decrease in velocity suggest an origin in a low-density

https://doi.org/10.1038/s41550-025-02725-1

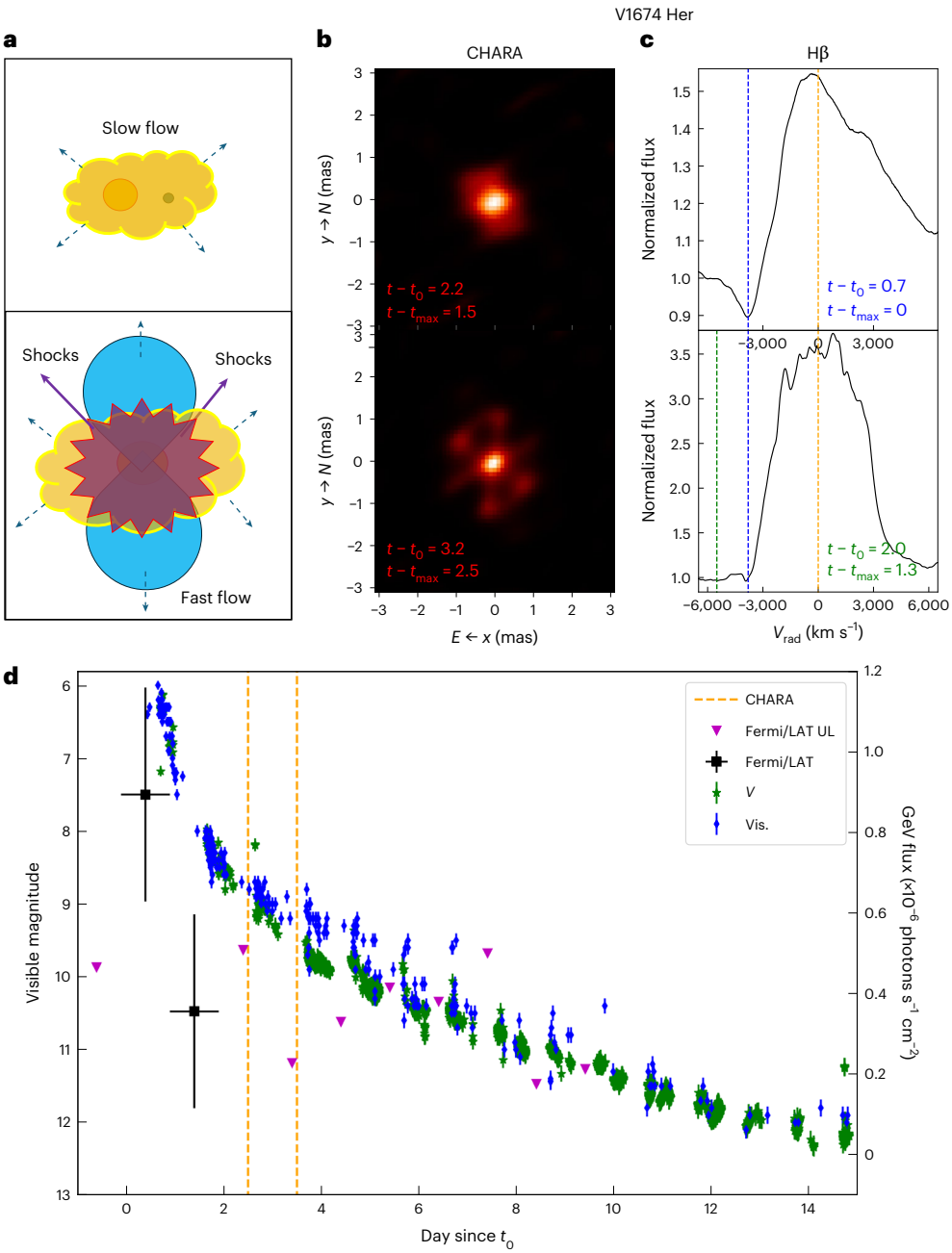

Fig. 1 | Early imaging of nova V1674 Her reveals a shift from spherical symmetry with potential multiple outflows. a, Multiple-ejection schematic illustration—an early slower flow followed near optical peak by a faster outflow; their collision produces GeV γ-ray-emitting shocks (purple arrows). **b**, CHARA images at $t = 2.2$ and 3.2 days after discovery (t_0 = 2021 June 12.19 UT; Supplementary Information), reconstructed with BSMEM (Methods). The images show a central elongated component surrounded by an extended structure elongated roughly perpendicular to it; we interpret the inner feature as the slow flow and the extended feature as the fast outflow. **c**, Hβ spectral line profiles taken on days 0.7 and 2 since t_0. The dashed orange, blue and green lines represent $v_{rad} = 0$ km s^{-1}, −3,800 km s^{-1} and −5,500 km s^{-1} relative to rest wavelength, respectively. **d**, The AAVSO visible (green stars for *V*-band and blue points for visual measurements, noted Vis.) and GeV γ-rays (black squares for detections and magenta triangles for 1σ upper limits, noted UL in the legend) light curves of V1674 Her. The error bars represent 1 − σ uncertainties. The vertical dashed lines represent the dates of the CHARA imaging.

wind emanating from the system during the premaximum halt. While most novae show a premaximum halt during the rise to visible peak, this halt could last between a few hours in fast novae and up to several weeks in slowly evolving novae[48,49].

After this first peak, V1405 Cas was detected as a GeV source detected by Fermi (more than 2 months into the eruption), implying the presence of strong energetic shocks within the nova ejecta[50]. This also implies that the shock onset appears delayed by more than 2 months after the outburst (in contrast to the case of V1674 Her where GeV emission was detected after less than a day), raising questions about the mass-loss history—whether a substantial part of the envelope was ejected late and/or subsequent winds from the white dwarf were launched only after a substantial delay.

The nova stayed bright for more than 200 days, showing multiple flares or maxima where the nova colours show substantial changes (Supplementary Fig. 16). It then gradually dimmed in the visible over several months (see the full light curve in Supplementary Fig. 14). Such slow evolution is the antithesis of V1674 Her's rapid eruption, emphasizing the diversity of nova ejection mechanisms and the complexity of mass-loss processes.

https://doi.org/10.1038/s41550-025-02725-1

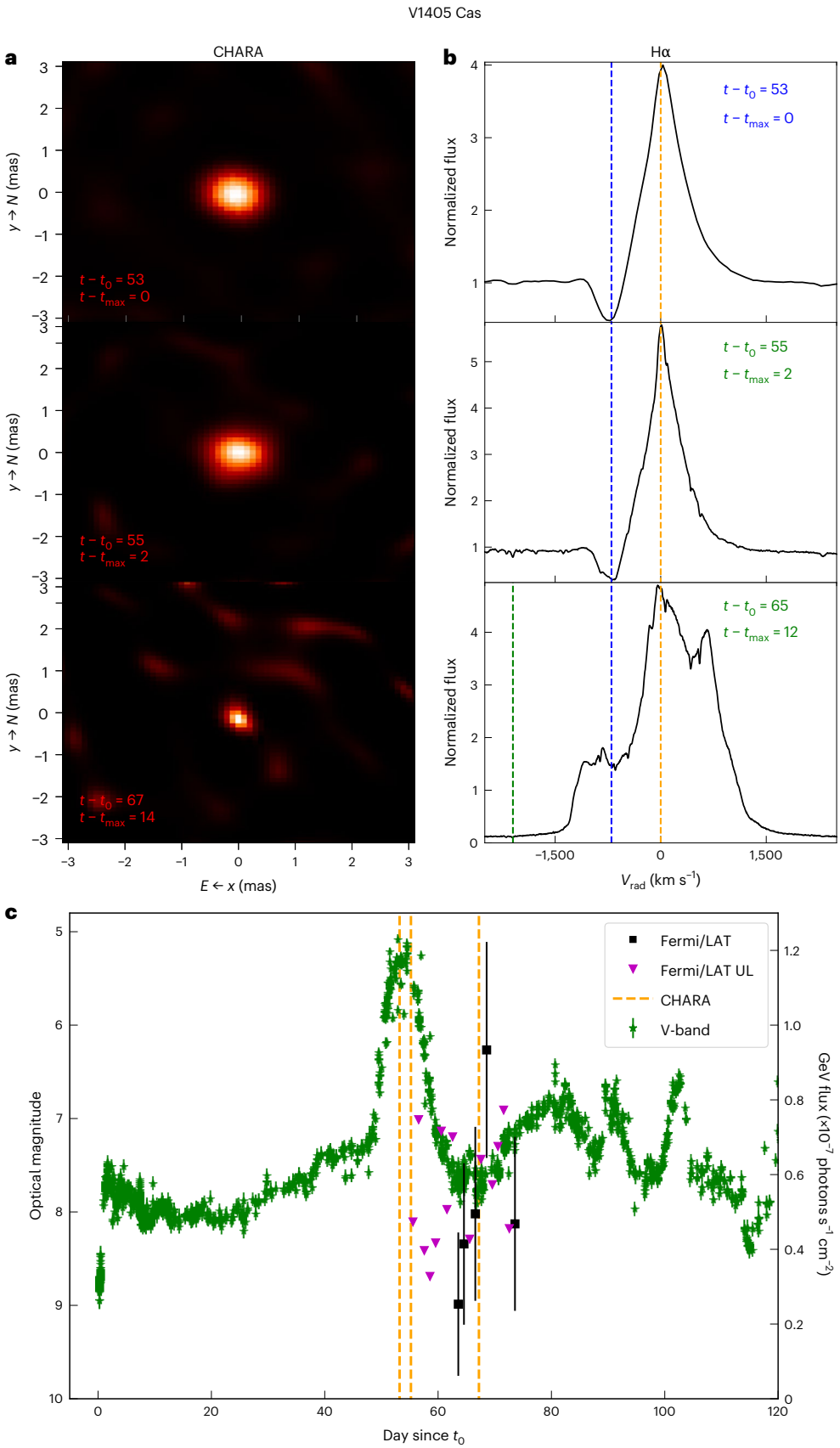

Fig. 2 | Early imaging of nova V1405 Cas reveals a delay in ejection of more than 50 days into eruption. a, Three CHARA images obtained on days 53, 55 and 67 since t_0, reconstructed with BSMEM (Methods). **b**, Hα spectral line profiles taken on days 53, 55 and 65, since t_0. The dashed orange, blue and green dashed lines represent $v_{rad} = 0$ km s^{-1}, −700 km s^{-1} and −2,100 km s^{-1} relative to rest wavelength, respectively. **c**, The AAVSO *V*-band (green stars) and GeV γ-ray (black squares for detections and magenta triangles for 1σ upper limits, noted UL in the legend) light curves of V1405 Cas (Methods). The error bars represent 1 − σ uncertainties. The vertical dashed lines represent the dates of the CHARA epochs.

Several slow novae have been observed to exhibit a similarly long-lasting premaximum halt, followed by a gradual rise to the visible peak over several weeks[49,51–53], the origins of which have not been fully understood yet. Nevertheless, a few ideas have been proposed, some of which suggested that, during this early rise to visible peak, the binary motion might play a role in driving the mass loss and eventually expelling the nova envelope (for example, refs. 28,54), during a short but important phase of common-envelope interaction (see Supplementary Information for more details). With the new insights brought by the presence of strong, energetic shocks during the early days and weeks of a nova, emphasis on the role of the binary motion in driving the mass loss and expelling the nova envelope has gained traction more recently (for example, refs. 3,10). However, direct observational evidence for delayed ejection of the bulk of the nova envelope and the potential role of the binary motion in driving the mass loss in novae is still lacking. Therefore, resolved imaging of slowly evolving novae such as V1405 Cas during their peak brightness can substantially improve our understanding of the role of the binary in driving the mass loss in novae.

Motivated by these findings, we obtained two CHARA observations of nova V1405 Cas near its visible peak, and a third observation 2 weeks later (approximately 53, 55 and 67 days after discovery; approximately 0, 2 and 14 days from peak, respectively). Surprisingly, the first two observations showed a resolved central source with little to no ejecta around it (Fig. 2). In these two images, the central source accounts for more than 95% of the emission, whereas any potential extended structure contributes only a few per cent. This extended component is possibly responsible for the premaximum P Cygni profiles observed during the rise to peak brightness (Fig. 2b and Supplementary Fig. 20).

The diameter of the resolved central source in the first CHARA epoch is 0.99 ± 0.02 mas (Supplementary Figs. 25–27 and Supplementary Table 5). Using a distance of 1.73 kpc measured by Gaia (Supplementary Information), this translates to a source size of around 1.71 AU (that is, a radius of around 0.85 AU), meaning that the size of the emitting photosphere, in the H-band, is indeed similar to that of a red giant star. If the nova envelope was impulsively ejected at t_0 and expanded for 53 days with velocities ranging between 700 km s^{-1} and 1,500 km s^{-1} (as measured from the troughs of the P Cygni profiles in the optical and infrared spectra before peak brightness; Supplementary Figs. 19 and 20), then the line-emitting region should have a size between 23 AU and 46 AU at visible peak. Although the size of the line-emitting regions is not necessarily representative of the continuum-emitting region, at peak brightness it should give us a rough estimate of the size of the photosphere (responsible for the majority of the emission), implying that the majority of the emission should be originating in an extended structure (which would be resolved out by CHARA).

The large discrepancy between the expected radius of the photosphere (~23–46 AU, if the envelope is impulsively ejected at the beginning of the eruption) and the measured radius of the emitting source responsible for the majority of the emission (~0.85 AU), suggests that the bulk of the nova envelope is not fully expelled 53–55 days into the eruption—indicating a delayed ejection of the envelope.

In the third epoch, there is a remarkable change in the structure of the system and the origin of the emission: the central source is now responsible for only ~45–50% of the emission, while the rest of the emission is originating in an extended structure, which is resolved out by CHARA. At this stage, the nova also shows: (1) a broad emission component characterized by a half width at zero intensity of around 2,100 km s^{-1} in the optical spectral lines, (2) GeV γ-ray emission detected by Fermi-LAT (see ref. 50 and Fig. 2) and (3) hard X-ray emission originating in shock-heated plasma detected by the Neil Gehrels Swift Observatory 5 days after the third CHARA epoch (see Supplementary Fig. 15). The expansion or expulsion of the nova envelope may be driven by multiple mechanisms. The faster outflows observed in the optical spectral can plow into the puffed-up envelope, helping it to escape the system. Such interaction could lead to energetic shocks, which power high-energy emission (detected by Swift and Fermi)—again, in agreement with the multiple-outflow scenario suggested to explain shocks in novae. In addition, the binary orbital motion can also play an important role in expelling the bulk of the puffed-up envelope. References [9,28] argued that the binary motion could transfer angular momentum and energy to the ejecta, which might help expel the nova envelope.

Moreover, the imaged central source shrinks in size between the second and third epoch, which is consistent with the density of the material near the binary dropping. Based on the above, we conclude that the bulk of the nova envelope probably continued to engulf the binary system for more than 50 days in a common-envelope phase during the rise to peak visible brightness, and was only expelled after more than 55 days, eventually leading to shock interactions, as indicated by the delayed detection of high-energy emission.

After the first visible peak, the light curve of V1405 Cas exhibits multiple flares (at least nine) over a period exceeding 200 days, with some reaching amplitudes greater than 2 magnitudes (Supplementary Fig. 14). During the flaring activity, new absorption features in the spectra appear at progressively higher velocities (Supplementary Figs. 17, 18 and 20–24). This suggests that the multiple flares may result from renewed mass-ejection episodes, with new material launched at increasingly faster velocities. As faster material catch up with previously ejected slower material, further shock interaction manifests, contributing to the nova's multiwavelength emission[18,55,56]. This underscore the complexity of mass-loss processes during nova eruptions.

In summary, our results highlight the potential role of the binary motion in driving mass-loss in novae[3,10,54] and encourage future theoretical studies and modelling to explore this role. They also provide observational evidence for a delayed ejection of the bulk of the envelope during a nova, indicating that nova ejections are more complex than a single, impulsive event at the start of the eruption. By increasing the sample of novae observed with CHARA and other optical and NIR interferometers in the future, we can confirm if this delayed ejection is common in other novae, which would establish novae as ideal laboratories in our Galactic backyard to constrain the physics of common-envelope interaction.

Methods

CHARA NIR interferometry

We utilized the Georgia State University CHARA Array[36] to observe nova V1674 Her on UT 2021 June 14 and 15 (days 2 and 3) and nova V1405 Cas on UT 2021 May 10, 12 and 24 (days 53, 55 and 67), to probe angular scales with submilliarcsecond resolution using the method of NIR interferometry. The Michigan InfraRed Combiner – eXeter (MIRC-X[45]) combines the light from all six CHARA telescopes simultaneously in the NIR H-band (typical λ_0 = 1.62 μm, $\Delta\lambda$ = 0.25 μm), providing sufficient Fourier space (u,v) coverage for simple interferometric imaging. The observations of nova V1674 Her combined all six telescopes using the PRISM102 mode with a spectral resolving power of $R \approx 102$. The observations of V1405 Cas used only five telescopes because the S1 telescope was not in delay. The observations used the GRISM190 mode on May 10 and 24 and the PRISM50 mode on May 12, providing spectral resolving powers of $R \approx 190$ and 50, respectively. In Supplementary Figs. 1 and 12, we present the CHARA (u,v) coverage for the different epochs. The raw data were reduced using the publicly available data pipeline[57] to produce visibility amplitudes on up to 15 baselines and closure phases on up to 20 closed triangles. We used an integration time of 30 s (ref. 58). The calibration of the instrumental transfer function required observations of single stars with known diameters estimated by SEARCHCAL[59–61]. We used a calibration script written in IDL by J. D. Monnier to average the measurements over 2.5-min intervals with the 'deep cleaning' option to remove outliers. For nova V1405 Cas, we used HD 211982 (0.570 ± 0.015 mas), HD 135969 (0.215 ± 0.006 mas), HD 145965 (0.211 ± 0.005 mas), HD 151259 (0.425 ± 0.011 mas) and HD 219080 (0.69 ± 0.069 mas). The calibrators on UT 2021 May 12 were

located at a declination of −23° at a very large angular separation on sky from V1405 Cas (declination +61°). For nova V1674 Her, we used HD 177433 (0.537 ± 0.012 mas) and HD 184607 (0.540 ± 0.012 mas). The calibrated OIFITS files are available through the JMMC Optical Interferometry Database[62]. The log of the CHARA observations is listed in Supplementary Tables 1 and 4.

At these early times in the evolution of the novae, we see some modest evidence (Supplementary Figs. 10 and 11) for small visibility changes across the spectrum when observed in medium resolution (R190), for instance due to strong hydrogen lines. However, the effect is relatively small (and hardly seen in the closure phase spectra), so we have combined all the spectral channels together for imaging, assuming grey emission. In the future, a more sophisticated treatment could account for the line emission as a separately imaged component, but for now we are interested in the overall geometrical changes during the first few weeks of the main continuum emission (first few weeks of the eruption).

For the CHARA aperture synthesis imaging presented here, we used a maximum entropy imaging algorithm that is directly fitted to the V^2 and closure phase quantities, first described by ref. 63 and later implemented in a publicly available package called the BI-SPECTRUM MAXIMUM ENTROPY METHOD (BSMEM)[64]. We used BSMEM (v1.5) to fit to OIFITS data that were averaged on 15-min timescales. To provide a prior for BSMEM, an elliptical Gaussian was fitted to the visibility data for each epoch. All imaging presented used the same BSMEM settings: pixel scale 0.1 mas, width 64 × 64 pixels, constrained V^2 at origin to 1.00 ± 0.05, Gaussian elliptical prior, maximum 50 iterations, and regularization hyperparameter evaluation using classical Bayesian with known noise scale (−*rt*1). For more discussion on our approach to imaging with NIR interferometry data, see the overview in ref. 65.

Our results are shown in Supplementary Figs. 2 and 13. Each column shows a different epoch. The top row for each nova shows the prior image used based on an elliptical Gaussian fit to the visibility data. The middle row shows the BSMEM image using a linear scale. We also include in the middle panel the percentage of the flux contained within 1 mas of the brightest pixel. The bottom row shows the square-root intensity, to highlight low-surface brightness emission within the field of view.

We note a few further details here. The bright spots around the ring for nova V1674 Her on day 3 are probably due to the limited CHARA baselines; the visibility data themselves are consistent with a more continuous, elongated ring, with brightness varying with azimuth and peaking along the diagonal; Supplementary Information). For the final epoch of nova V1405 Cas on day 63, about 50% of the flux is overresolved, but we lack short baselines to make a reliable image; thus, the spots in the background are probably artefacts from a diffuse low-surface brightness shell with scale >5 mas. This epoch also showed signs of line emission in the H-band spectrum, and we also carried out imaging limiting to 1.5–1.6 μm, avoiding most of the strong emission lines. These results were consistent with those from the full spectrum, albeit with lower reduced chi-squared values, and were therefore not shown in Supplementary Figs. 2 and 13 for clarity.

Optical and infrared spectroscopy and photometry

We obtained optical spectra for novae V1674 Her and V1405 Cas using a diversity of facilities and instruments. In Supplementary Tables 3 and 6, we list the log of these observations. Below we summarize the observations and data reduction.

We have used the Gemini-North Multi-Object Spectrograph[66] on the 8.1-m Gemini-North to observe nova V1674 Her on 2021-06-17, 06-19, 06-27, 07-01, 07-04, 07-07 and 07-09 (days 5, 7, 15, 19, 22, 25 and 27). The observations were taken using the 0.5″ slit and the R831 grating to provide a range of 4,500–6,800 Å at a resolving power $R \approx 4{,}400$). The Gemini Multi-Object Spectrograph spectra were reduced with the aid of DRAGONS v3.1.0[67], applying bias subtraction and flat fielding, and establishing a wavelength solution based on the arc spectra. Because the latter were obtained during daytime, the zero point of the wavelength solution was checked for instrument flexure by measuring the Oxygen 5577.33 Å sky emission. Deviations were found to be at most 0.1 Å and were corrected when necessary.

Optical spectra were obtained for nova V1674 Her with the SuperNova Integral Field Spectrograph[68] on the University of Hawaii UH2.2m telescope through the Spectroscopic Classification of Astronomical Transients[69] survey. The SuperNova Integral Field Spectrograph is an integral field unit covering 3,400–9,000 Å at $R \approx 1{,}000$ over a 6′ × 6′ field of view with a spatial sampling of 0.4 arcsec per spaxel. The two-dimensional frames are converted into three-dimensional (x, y, λ) datacubes, flat-fielded with a continuum lamp exposure and extracted into a one-dimensional spectrum by applying aperture photometry to each wavelength slice. Spectra are then corrected for the optical system throughput and atmospheric extinction[70] using observations of spectrophotometric standard stars[71]. Reference 69 provides a detailed description of the processing pipeline.

We make use of publicly available spectra reported to the Astronomical Ring for Access to Spectroscopy (ARAS)[72]. The data consist of a combination of low-resolution ($R \approx 1{,}000$), medium-resolution and high-resolution (up to $R \approx 20{,}000$) spectra obtained by citizen scientists.

On 2021 March 23.13 and 28.12 UT (days 5 and 10 since t_0), we obtained observations of nova V1405 Cas using the Visible and Near-Infrared Imaging Spectrograph mounted on the 1.0-m telescope of the Aerospace Corporation. A description of the telescope is given in ref. 73. The raw spectra were compensated for atmospheric absorption and converted to absolute flux using observations of the G-type standard stars Hip 63333 and Hip 2087.

We make use of publicly available data reported to the American Association of Variable Stars (AAVSO)[74] to create the optical light curves for both novae. The data consist of blue (B), visible (V), red (R), and infrared (I) photometry and visual (Vis.) estimates.

Fermi-LAT γ-ray observations and analysis

We downloaded the Fermi Pass 8 γ-ray data (P8R3_V3) of V1674 Her and V1405 Cas from the LAT Data Server. The obtained data cover an energy range from 100 MeV to 300 GeV within circular regions of radius 10° centred on the targets. The standard analysis software, Fermitools (version 2.2.0), was used for the LAT data reduction and analysis. Only type 3 data (front and back conversion types) in the event class 128 (standard source class) were used. As Earth's limb is a bright source of γ-rays that influences the LAT observations, events with apparent zenith angle larger than 90° are removed. We also excluded the time periods with bad data quality flags to obtain good time intervals.

Daily γ-ray light curves of the novae were extracted using the binned likelihood method. Note that MJD 59339 had a problem, so no data were available on this day. To solve this, we fixed the isotropic background emission and extended the analysis day from 1 day to 1.1 days. In the analysis, emission model files were built for the fields based on the spatial and spectral information of the 4FGL-DR3 catalogued sources located within 20° from the targets[75]. The γ-ray spectra of both novae were assumed to follow a simple power-law model for simplicity. Except for the normalization factors of the novae, all the spectral parameters in the model file including the Galactic diffuse and isotropic emission (that is, gll_iem_v07 and iso_P8R3_SOURCE_V3_v1) were fixed to the 4FGL-DR3 best-fit values to avoid overfitting due to the low-count statistics. For V1674 Her, the implied (best-fit) photon index is −2.3 and the emission was active on 2021 June 12 and 13 (during the first day since t_0 (ref. 76)). To estimate the photon index of V1405 Cas, we first extracted a preliminary γ-ray light curve with a fixed photon index. We defined the γ-ray active phase by the first and last dates with TS $\gtrsim$4 over a 24-h period (where TS is the likelihood ratio test statistic) in the light curve. This interval of data was then reanalysed using the likelihood method to

obtain the best-fit photon index, which is −2.74 ± 0.23 in the period from 2021 May 21 to June 2 (days 64–76 after eruption). Binned likelihood fitting was then performed daily for both novae from 2021 March 18 to June 9. For those daily bins with significant detections (that is, TS $\gtrsim$4, over a 24-h period), the inferred photon fluxes with $1-\sigma$ uncertainties are presented (where σ represents the standard deviation). Otherwise, 95% upper limits are reported.

Swift XRT and UVOT observations

The Neil Gehrels Swift Observatory (Swift) observations of V1405 Cas began on 2021 March 24, 5.6 days after the discovery, with exposures initially obtained every 3 days, with the cadence subsequently dropping to weekly and then fortnightly until the end of 2021 June. The data have been downloaded from the UK Swift Science Data Centre.

The Swift X-ray Telescope (XRT) data were processed with the standard HEASOFT analysis software, together with the corresponding calibration files. Given the brightness of the ultraviolet/optical emission, only grade 0 (single-pixel X-ray events) were considered in this work to minimize contamination from optical loading[77]. Upon this more detailed examination, the XRT detection reported in ref. 78 (using grade 0–12 multipixel events) was determined to be spurious. During the first 3 months following the eruption, the vast majority of the Swift datasets did not show significant X-ray detections, and so 3σ upper limits are reported in Supplementary Fig. 15. However, the observations on 2021 May 31 and June 15 (days 74 and 89 since t_0) did reveal an X-ray source at the location of the nova. Detailed checks show that the spectrum of this source is inconsistent with optical loading: the combined emission from the two detections can be approximated with a single-temperature optically thin thermal plasma of $kT > 2.6$ keV (where k is the Boltzmann constant and T is the temperature in Kelvin, so their product kT represents the thermal energy per particle), assuming an absorbing column $N_{\rm H} = 3.8 \times 10^{21}$ cm^{-2} (ref. 78), providing an observed (unabsorbed) flux estimate of 1.2 (1.5) $\times 10^{-12}$ erg cm^{-2} s^{-1} over 0.3–10 keV. Because 'false' X-rays from optical loading would appear much softer, the X-ray detections on these 2 days are therefore considered to be real. Subsequent observations from 2021 June 30 to July 30 (days 104–134) did not show significant X-ray emission; however, the upper limits on the count rates are consistent with the two detections.

The Swift UltraViolet and Optical Telescope (UVOT) obtained photometry in three ultraviolet filters: $uvw2$, $uvm2$ and $uvw1$ centred around 190, 220 and 260 nm, respectively. Due to the brightness of the source, the calibration of the readout streak[79] was used with the UVOTPY[80] software.

Data availability

The data used in this article are available via figshare at https://doi.org/10.6084/m9.figshare.30330472 (ref. 81).

References

1. Gallagher, J. S. & Starrfield, S. On the total energy output of the nova outburst. *Mon. Not. R. Astron. Soc.* **176**, 53–61 (1976).
2. Starrfield, S. in *Classical Novae of Cambridge Astrophysics Series, No. 43* (eds Bode, M. F. & Evans, A.) 39–60 (Wiley, 1989).
3. Shen, K. J. & Quataert, E. Binary interaction dominates mass ejection in classical novae. *Astrophys. J.* **938**, 31 (2022).
4. McLaughlin, D. B. The behaviour of absorption systems in spectra of novae. *Ann. d'Astrophys.* **27**, 450 (1964).
5. Aydi, E. et al. Early spectral evolution of classical novae: consistent evidence for multiple distinct outflows. *Astrophys. J.* **905**, 62 (2020).
6. Friedjung, M. The physics of the nova phenomenon. *Mon. Not. R. Astron. Soc.* **131**, 447–462 (1966).
7. Friedjung, M. The formation of the principal system of novae. *Astron. Astrophys.* **180**, 155–159 (1987).
8. Friedjung, M. Do novae have optically thick winds during outburst with large deviations from spherical symmetry? *Astron. Astrophys.* **536**, A97 (2011).
9. Livio, M. Classical novae and the extragalactic distance scale. *Astrophys. J.* **393**, 516–522 (1992).
10. Chomiuk, L. et al. Binary orbits as the driver of γ-ray emission and mass ejection in classical novae. *Nature* **514**, 339–342 (2014).
11. Ackermann, M. et al. Fermi establishes classical novae as a distinct class of gamma-ray sources. *Science* **345**, 554–558 (2014).
12. Cheung, C. C. et al. Fermi-LAT gamma-ray detections of classical novae V1369 Centauri 2013 and V5668 Sagittarii 2015. *Astrophys. J.* **826**, 142 (2016).
13. Franckowiak, A., Jean, P., Wood, M., Cheung, C. C. & Buson, S. Search for gamma-ray emission from Galactic novae with the Fermi-LAT. *Astron. Astrophys.* **609**, A120 (2018).
14. Chomiuk, L., Metzger, B. D. & Shen, K. J. New insights into classical novae. *Annu. Rev. Astron. Astrophys.* **59**, 391–444 (2021).
15. Metzger, B. D. et al. Shocks in nova outflows—I. Thermal emission. *Mon. Not. R. Astron. Soc.* **442**, 713–731 (2014).
16. Metzger, B. D. et al. Gamma-ray novae as probes of relativistic particle acceleration at non-relativistic shocks. *Mon. Not. R. Astron. Soc.* **450**, 2739–2748 (2015).
17. Li, K.-L. et al. A nova outburst powered by shocks. *Nat. Astron.* **1**, 697–702 (2017).
18. Aydi, E., Chomiuk, L., Sokolovsky, K. V. & Steinberg, E. Direct evidence for shock-powered optical emission in a nova. *Nat. Astron.* **2**, 697–702 (2020).
19. Chevalier, R. A. & Irwin, C. M. Shock breakout in dense mass loss: luminous supernovae. *Astrophys. J. Lett.* **729**, L6 (2011).
20. Silverman, J. M. et al. Type Ia supernovae strongly interacting with their circumstellar medium. *Astrophys. J. Suppl. Ser.* **207**, 3 (2013).
21. Metzger, B. D. & Pejcha, O. Shock-powered light curves of luminous red novae as signatures of pre-dynamical mass-loss in stellar mergers. *Mon. Not. R. Astron. Soc.* **471**, 3200–3211 (2017).
22. Hachisu, I. & Kato, M. A strong shock during a nova outburst: an origin of multiple velocity systems in optical spectra and of high-energy emissions. *Astrophys. J.* **939**, 1 (2022).
23. Mclaughlin, D. B. Locations of origin of spectral features of novae. *Publ. Astron. Soc. Pac.* **59**, 244 (1947).
24. Payne-Gaposchkin, C. H. P. *The Galactic Novae* (North-Holland Publishing Co., 1957).
25. Friedjung, M. Physics of the nova phenomenon, II. *Mon. Not. R. Astron. Soc.* **132**, 143–181 (1966).
26. Friedjung, M. The physics of the nova phenomenon, III. *Mon. Not. R. Astron. Soc.* **132**, 317–336 (1966).
27. Friedman, S. D. et al. Studies of diffuse interstellar bands V. Pairwise correlations of eight strong DIBs and neutral hydrogen, molecular hydrogen, and color excess. *Astrophys. J.* **727**, 33 (2011).
28. Lloyd, H. M., O'Brien, T. J. & Bode, M. F. Shaping of nova remnants by binary motion. *Mon. Not. R. Astron. Soc.* **284**, 137–147 (1997).
29. Nebot Gómez-Morán, A. et al. Post common envelope binaries from SDSS. XII. The orbital period distribution. *Astron. Astrophys.* **536**, A43 (2011).
30. Ivanova, N. et al. Common envelope evolution: where we stand and how we can move forward. *Astron. Astrophys. Rev.* **21**, 59 (2013).
31. Schneider, F. R. N., Lau, M. Y. M. & Roepke, F. K. Stellar mergers and common-envelope evolution. Preprint at https://arxiv.org/abs/2502.00111 (2025).
32. O'Brien, T. J. et al. An asymmetric shock wave in the 2006 outburst of the recurrent nova RS Ophiuchi. *Nature* **442**, 279–281 (2006).

33. O'Brien, T. J. & Bode, M. F. in *Classical Novae* 2nd edn of Cambridge Astrophysics Series, No. 43 (eds Bode, M. F. & Evans, A.) 285–306 (Cambridge Univ. Press, 2008).
34. Lyke, J. E. & Campbell, R. D. The distance and morphology of V723 Cassiopeiae (Nova Cassiopeia 1995). *Astron. J.* **138**, 1090–1100 (2009).
35. Chesneau, O. et al. The expanding dusty bipolar nebula around the nova V1280 Scorpi. *Astron. Astrophys.* **545**, A63 (2012).
36. ten Brummelaar, T. A. et al. First results from the CHARA Array. II. A description of the instrument. *Astrophys. J.* **628**, 453–465 (2005).
37. Petrov, R. G. et al. AMBER, the near-infrared spectro-interferometric three-telescope VLTI instrument. *Astron. Astrophys.* **464**, 1–12 (2007).
38. GRAVITY Collaboration et al. First light for GRAVITY: phase referencing optical interferometry for the Very Large Telescope Interferometer. *Astron. Astrophys.* **602**, A94 (2017).
39. Chesneau, O. et al. The 2011 outburst of the recurrent nova T Pyxidis. Evidence for a face-on bipolar ejection. *Astron. Astrophys.* **534**, L11 (2011).
40. Schaefer, G. H. et al. The expanding fireball of Nova Delphini 2013. *Nature* **515**, 234–236 (2014).
41. Woodward, C. E. et al. Near-infrared studies of Nova V1674 Herculis: a shocking record breaker. *Astrophys. J. Lett.* **922**, L10 (2021).
42. Sokolovsky, K. V. et al. The multiwavelength view of shocks in the fastest nova V1674 Her. *Mon. Not. R. Astron. Soc.* **521**, 5453–5472 (2023).
43. Kato, M., Hachisu, I. & Saio, H. A comprehensive light-curve model of the Very Fast Nova V1674 Herculis. *Astrophys. J.* **988**, 112 (2025).
44. Hachisu, I. & Kato, M. Optical detection of the X-ray flash in the Very Fast Nova V1674 Her: optical contribution of the irradiated accretion disk. *Astrophys. J.* **989**, 153 (2025).
45. Anugu, N. et al. MIRC-X: a highly sensitive six-telescope interferometric imager at the CHARA Array. *Astron. J.* **160**, 158 (2020).
46. Habtie, G. R., Das, R., Pandey, R., Ashok, N. M. & Dubovsky, P. A. Study of the fastest classical nova, V1674 Her: photoionization and morpho-kinemetic model analysis. *Mon. Not. R. Astron. Soc.* **527**, 1405–1423 (2024).
47. Shore, S. N. The spectroscopic development of a nova. In *Stellar Novae: Past and Future Decades, Vol. 490 of Astronomical Society of the Pacific Conference Series* (eds Woudt, P. A. & Ribeiro, V. A. R. M.) 145 (Astronomical Society of the Pacific (ASP), 2014).
48. Warner, B. CP Puppis and V1500 Cygni. *Mon. Not. R. Astron. Soc.* **217**, 1P–5P (1985).
49. Strope, R. J., Schaefer, B. E. & Henden, A. A. Catalog of 93 nova light curves: classification and properties. *Astron. J.* **140**, 34–62 (2010).
50. Buson, S., Cheung, C. C. & Jean, P. Fermi-LAT gamma-ray detection of Nova V1405 Cas 2021. *Astron. Telegram* **14658**, 1 (2021).
51. Munari, U. et al. Spectroscopy and UBVR_J_-JHKLM photometry of Nova Cassiopeiae 1995: the first 210 days. *Astron. Astrophys.* **315**, 166–169 (1996).
52. Hachisu, I. & Kato, M. The nature of premaximum halts of classical nova outbursts: V723 Cassiopeiae and V463 Scuti. *Astrophys. J. Lett.* **612**, L57–L60 (2004).
53. Kato, T. & Takamizawa, K. Nova Aql 2001: another V723 Cas-type slow nova? *Inf. Bull. Variable Stars* **5100**, 1 (2001).
54. Livio, M., Shankar, A., Burkert, A. & Truran, J. W. The common envelope phase in the outbursts of classical novae. *Astrophys. J.* **356**, 250–254 (1990).
55. Pejcha, O. Time-dependent rebrightenings in classical nova outbursts: a late-time episodic fuel burning? *Astrophys. J. Lett.* **701**, L119–L122 (2009).
56. Aydi, E. et al. Flaring, dust formation, and shocks in the Very Slow Nova ASASSN-17pf (LMCN 2017-11a). Preprint at https://arxiv.org/abs/1903.09232 (2019).
57. Le Bouquin, J.-B. mircx_pipeline. *Gitlab* https://gitlab.chara.gsu.edu/lebouquj/mircx_pipeline (2017).
58. Monnier, J. D. Phases in interferometry. *New Astron. Rev.* **51**, 604–616 (2007).
59. Bonneau, D. et al. SearchCal: a Virtual Observatory tool for searching calibrators in optical long-baseline interferometry. II. The faint-object case. *Astron. Astrophys.* **535**, A53 (2011).
60. Bourgés, L. et al. The JMMC Stellar Diameters Catalog v2 (JSDC): a new release based on SearchCal improvements. In *Astronomical Data Analysis Software and Systems XXIII, Vol. 485 of Astronomical Society of the Pacific Conference Series* (eds Manset, N. & Forshay, P.) 223 (Astronomical Society of the Pacific (ASP), 2014).
61. Chelli, A. et al. Pseudomagnitudes and differential surface brightness: application to the apparent diameter of stars. *Astron. Astrophys.* **589**, A112 (2016).
62. OiDB. *JMMC* https://www.jmmc.fr/english/tools/data-bases/oidb/ (2014).
63. Buscher, D. F. in *Very High Angular Resolution Imaging* Vol. 158 (eds Robertson, J. G. & Tango, W. J.) 91 (Springer, 1994).
64. Malbet, F. et al. The 2010 interferometric imaging beauty contest. In *Optical and Infrared Interferometry II, Vol. 7734 of Proc. SPIE* (eds Danchi, W. C. et al.) 77342N (The International Society for Optics and Photonics (SPIE), 2010).
65. Baron, F. Image reconstruction in optical interferometry: an up-to-date overview. In *Astronomy at High Angular Resolution, Vol. 439 of Astrophysics and Space Science Library* (eds Boffin, H. M. J. et al.) 75 (Springer, 2016).
66. Hook, I. M. et al. The Gemini-North Multi-Object Spectrograph: performance in imaging, long-slit, and multi-object spectroscopic modes. *Publ. Astron. Soc. Pac.* **116**, 425–440 (2004).
67. Labrie, K., Anderson, K., Cárdenes, R., Simpson, C. & Turner, J. E. H. DRAGONS—Data Reduction for Astronomy from Gemini Observatory North and South. In *Astronomical Data Analysis Software and Systems XXVII, Vol. 523 of Astronomical Society of the Pacific Conference Series* (eds Teuben, P. J. et al.) 321 (Astronomical Society of the Pacific (ASP), 2019).
68. Lantz, B. et al. SNIFS: a wideband integral field spectrograph with microlens arrays. In *Optical Design and Engineering, Vol. 5249 of Proc. SPIE* (eds Mazuray, L. et al.) 146–155 (The International Society for Optics and Photonics (SPIE), 2004).
69. Tucker, M. A. et al. The Spectroscopic Classification of Astronomical Transients (SCAT) survey: overview, pipeline description, initial results, and future plans. *Publ. Astron. Soc. Pac.* **134**, 124502 (2022).
70. Buton, C. et al. Atmospheric extinction properties above Mauna Kea from the Nearby SuperNova Factory spectro-photometric data set. *Astron. Astrophys.* **549**, A8 (2013).
71. Rubin, D. et al. Uniform recalibration of common spectrophotometry standard stars onto the CALSPEC system using the SuperNova Integral Field Spectrograph. *Astrophys. J. Suppl. Ser.* **263**, 1 (2022).
72. Teyssier, F. Eruptive stars monitoring and the ARAS database. *Contrib. Astron. Observ. Skalnate Pleso* **49**, 217–227 (2019).
73. Rudy, R. J. et al. The coronal line spectrum of the Iron Nova V3666 Ophiuchi. *Astron. J.* **161**, 291 (2021).
74. Kloppenborg, B. K. Observations from the AAVSO International Database. *AAVSO* https://www.aavso.org (2023).
75. Abdollahi, S. et al. Incremental Fermi Large Area Telescope Fourth Source Catalog. *Astrophys. J. Suppl. Ser.* **260**, 53 (2022).
76. Lin, L. C.-C., Fan, J.-L., Hu, C.-P., Takata, J. & Li, K.-L. Investigation of a likely orbital periodicity of Nova Hercules 2021 in X-rays and γ-rays. *Mon. Not. R. Astron. Soc.* **517**, L97–L101 (2022).

77. Optical loading. *University of Leicester* https://www.swift.ac.uk/analysis/xrt/optical_loading.php (2012).
78. Sokolovsky, K. V. et al. Early NuSTAR and Swift X-ray detection of Nova Cassiopeiae 2021 = V1405 Cas = PNV J23244760+6111140. *Astron. Telegram* **14530**, 1 (2021).
79. Page, M. J. et al. The use and calibration of read-out streaks to increase the dynamic range of the Swift Ultraviolet/Optical Telescope. *Mon. Not. R. Astron. Soc.* **436**, 1684–1693 (2013).
80. Kuin, P. UVOTPY: Swift UVOT grism data reduction. Astrophysics Source Code Library (ASCL), record ascl:1410.004. *Astrophysics Source Code Library (ASCL)* http://ascl.net/1410.004 (2014).
81. Aydi, E. Online material for Aydi et al. 2025: multiple outflows and delayed ejections revealed by early imaging of novae. *figshare* https://doi.org/10.6084/m9.figshare.30330472 (2025).

Acknowledgements

This work was completed using support from NASA award 13-Fermi 80NSSC20K01237. This work is based upon observations obtained with the Georgia State University CHARA Array at Mount Wilson Observatory. Time at the CHARA Array was granted through the NOIRLab community access programme (NOIRLab PropID: 2021A-0042; PI: E.A.). The CHARA Array is supported by the National Science Foundation under grant nos. AST-2034336 and AST-2407956. Institutional support has been provided from the GSU College of Arts and Sciences and the GSU Office of the Vice President for Research and Economic Development. E.A. acknowledges support by NASA through the NASA Hubble Fellowship grant HST-HF2-51501.001-A awarded by the Space Telescope Science Institute, which is operated by the Association of Universities for Research in Astronomy, Inc., for NASA, under contract NAS5-26555. L.C. acknowledges NSF awards AST-1751874 and AST-2107070, NASA awards 80NSSC23K0497, 80NSSC23K1247 and 80NSSC25K7334, and a Cottrell fellowship of the Research Corporation. J.S. was supported by the Packard Foundation. J.L.S. is supported by NASA grants 80NSSC25K7082 and 80NSSC25K7068. M.O. acknowledges support from Chandra award GO2-23013X. M.O.-H. was supported by the Polish National Science Center grant 2019/32/C/ST9/00577 and the 'Initiative of Excellence - Research University' (ID-UB) programme at A. Mickiewicz University in Poznań. K.L.P. and N.P.M.K. acknowledge funding from the UK Space Agency. B.D.M. acknowledges support by NASA through the ATP programme (80NSSC22K0807), the Fermi Guest Investigator Program (grant number 80NSSC24K0408) and the Simons Foundation (grant number 727700). The Flatiron Institute is supported by the Simons Foundation. K.J.S. acknowledges support by NASA through the ATP programme (80NSSC20K0544). S.K. acknowledges support from an UK Science and Technology Facilities Council Small Award (ST/Y002695/1). We thank the ARAS and AAVSO observers from around the world who contributed their spectra to the ARAS database and their magnitude measurements to the AAVSO International Database, used in this work. S.K. acknowledges funding for MIRC-X from the European Research Council (ERC) under the European Union's Horizon 2020 research and innovation programme (Starting Grant No. 639889 and Consolidated Grant No. 101003096). J.D.M. acknowledges funding for the development of MIRC-X (NASA-XRP NNX16AD43G, NSF-AST 2009489) and MYSTIC (NSF-ATI 1506540, NSF-AST 1909165). This research has made use of the Jean-Marie Mariotti Center Aspro and SearchCal services. J.T.H. was supported by NASA grant 80NSSC23K1431.

Author contributions

E.A. wrote the text. E.A., J.D.M, A.M., G.H.S., M.O.-H., R.S., M.T., K.L.L., J.-L.F., K.L.P., N.P.M.K. and R.R. obtained and reduced the data, and contributed analysis to the paper. All authors contributed to the interpretation of the data and commented on the final paper.

Competing interests

The authors declare no competing interests.

Additional information

Supplementary information The online version contains supplementary material available at https://doi.org/10.1038/s41550-025-02725-1.

Correspondence and requests for materials should be addressed to Elias Aydi or John D. Monnier.

Peer review information *Nature Astronomy* thanks the anonymou(s) reviewers for their contribution to the peer review of this work.

Elias Aydi[1,2] ✉, John D. Monnier[3] ✉, Antoine Mérand[4], Gail H. Schaefer[5], Laura Chomiuk[2], Magdalena Otulakowska-Hypka[6], Jhih-Ling Fan[7], Kwan Lok Li[7], Kirill V. Sokolovsky[8], Ricardo Salinas[9], Michael Tucker[10,11,12], Benjamin Shappee[12], Richard Rudy[13], Kim L. Page[14], N. Paul M. Kuin[15], David A. H. Buckley[16,17], Peter Craig[2], Luca Izzo[18,19], Justin Linford[20], Brian D. Metzger[21,22], Koji Mukai[23,24], Marina Orio[25,26], Ken J. Shen[27], Jay Strader[2], Jennifer L. Sokoloski[21], Robert E. Williams[28,29], Montana N. Williams[30], Gesesew R. Habtie[31], Stefan Kraus[32], Narsireddy Anugu[5], Jean-Baptiste Le Bouquin[33], Sorabh Chhabra[32], Isabelle Codron[32], Tyler Gardner[34], Mayra Gutierrez[3], Noura Ibrahim[3], Cyprien Lanthermann[5], Benjamin R. Setterholm[35], Christopher Ashall[12], Jason T. Hinkle[12], Thomas de Jaeger[36] & Anna V. Payne[29]

[1]Department of Physics and Astronomy, Texas Tech University, Lubbock, TX, USA. [2]Center for Data Intensive and Time Domain Astronomy, Department of Physics and Astronomy, Michigan State University, East Lansing, MI, USA. [3]Astronomy Department, University of Michigan, Ann Arbor, MI, USA. [4]European Southern Observatory, Garching, Germany. [5]The CHARA Array of Georgia State University, Mount Wilson Observatory, Mount Wilson, CA, USA. [6]Astronomical Observatory Institute, Faculty of Physics and Astronomy, Adam Mickiewicz University, Poznań, Poland. [7]Department of Physics, National Cheng Kung University, Tainan City, Taiwan. [8]Department of Astronomy, University of Illinois at Urbana-Champaign, Urbana, IL, USA. [9]Nicolaus Copernicus Astronomical Center, Polish Academy of Sciences, Warsaw, Poland. [10]Center for Cosmology and AstroParticle Physics, Columbus, OH, USA. [11]Department of Astronomy, The Ohio State University, Columbus, OH, USA. [12]Institute for Astronomy, University of Hawai'i, Honolulu, HI, USA. [13]Kookoosint Scientific, Camarillo, CA, USA. [14]School of Physics and Astronomy, University of Leicester, Leicester, UK. [15]University College London, Mullard Space Science Laboratory, Holmbury House, Dorking, UK. [16]South African Astronomical Observatory, Observatory, South Africa. [17]Department of Astronomy, University of Cape Town, Rondebosch, South Africa. [18]Osservatorio Astronomico di Capodimonte, INAF, Naples, Italy. [19]Niels Bohr Institute, University of Copenhagen, DARK, Copenhagen, Denmark. [20]National Radio Astronomy Observatory, Socorro, NM, USA. [21]Columbia Astrophysics Laboratory and Department of Physics, Columbia University, New York, NY, USA. [22]Center for Computational Astrophysics, Flatiron Institute, New York, NY, USA. [23]CRESST and X-ray Astrophysics Laboratory, NASA/GSFC, Greenbelt, MD, USA. [24]Department of Physics, University of Maryland, Baltimore County, Baltimore, MD, USA. [25]INAF – Osservatorio di Padova, Padua, Italy. [26]Department of Astronomy, University of Wisconsin, Madison, WI, USA. [27]Department of Astronomy and Theoretical Astrophysics Center, University of California, Berkelely, Berkeley, CA, USA. [28]Department of Astronomy and Astrophysics, University of California, Santa Cruz, Santa Cruz, CA, USA. [29]Space Telescope Science Institute, Baltimore, MD, USA. [30]Physics Department, New Mexico Tech, Socorro, NM, USA. [31]Department of Physics, Debre Berhan University, Debre Berhan, Ethiopia. [32]Astrophysics Group, Department of Physics and Astronomy, University of Exeter, Exeter, UK. [33]Institut de Planetologie et d'Astrophysique de Grenoble, Grenoble, France. [34]Cooperative Institute for Research in Environmental Sciences, 216 UCB, University of Colorado Boulder, Boulder, CO, USA. [35]Max-Planck-Institut für Astronomie, Heidelberg, Germany. [36]L'École Pour l'Informatique et les Techniques Avancées, EPITA, Le Kremlin-Bicêtre, France. ✉e-mail: eaydi@ttu.edu; monnier@umich.edu